Summary: Polystyrene-*block*-poly(methyl methacrylate) nanorods were prepared by wetting ordered porous alumina templates. We systematically investigated the diameter-dependence of their morphologies by varying the pore diameters of the templates from 400 nm down to 25 nm. If the pore diameter exceeds the period of the block copolymer, the pores accommodate a non-integer number of repeat periods. In case of smaller pores the occurrence of an ordered state could not be unambiguously verified.

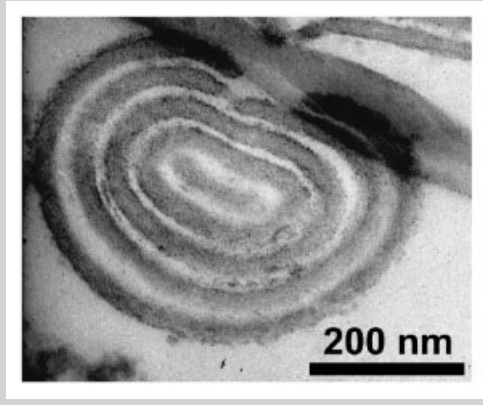

TEM image of an ultra-thin slice containing a cross-section of a polystyrene-*block*-poly(methyl methacrylate) nanorod embedded in epoxy resin.

Diameter-Dependence of the Morphology of PS-*b*-PMMA Nanorods Confined Within Ordered Porous Alumina Templates

Yiming Sun,[1,2] *Martin Steinhart,**[1] *Danilo Zschech,*[1] *Rameshwar Adhikari,*[2] *Goerg H. Michler,*[2] *Ulrich Gösele*[1]

[1] Max Planck Institute of Microstructure Physics, Weinberg 2, D-06120 Halle (Saale), Germany
Fax: +49 345 5511223; E-mail: steinhart@mpi-halle.de
[2] Department of Engineering, Institute of Materials Science, Martin Luther University Halle-Wittenberg, D-06099 Halle (Saale), Germany

Received: November 8, 2004; Revised: December 15, 2004; Accepted: December 16, 2004; DOI: 10.1002/marc.200400545

Keywords: block copolymers; interfaces; morphology; nanorods; nanotechnology

Introduction

Combining the intrinsic ability of block copolymers (BCPs) to form self-assembled mesoscopic structures[1] with the specific features of one-dimensional (1D) nano-objects is a promising access to miniaturised building blocks with complex internal morphologies. Thin BCP films[2] and wires[3] have already attracted considerable interest in the field of nanoscience. The use of porous materials as templates for the preparation of 1D nanostructures is a versatile and well-established technique.[4] The domain structure of polystyrene-*block*-polybutadiene (PS-b-PBD) BCP nanorods prepared by melting the BCPs into disordered porous alumina membranes has recently been investigated by Xiang et al.[5] It was found that in case of symmetric PS-b-PBD cylindrical lamellae, and in case of asymmetric PS-b-PBD cylinders of the minor phase, oriented parallel to the long axes of the pores, had been formed. The structure formation is strongly influenced by the wetting behaviour of the BCP components. When the pore wall is neutral with respect to both blocks the occurrence of a stacked-disk morphology with lamellae oriented normal to the pore axis has been predicted.[6,7] The morphology type reported by Xiang et al.[5], with PBD preferentially segregating to the interfaces, corresponds to the scenario where a non-neutral wall is present, i.e., one block shows a much stronger affinity to the pore walls than the other one. Even more sophisticated domain structures, such as stack-disk and toroidal ones have been reported by Shin et al.[8], indicating that a broad variety of exotic structures is accessible by adjusting the degree of geometric confinement, the BCP period and the BCP/wall interactions.

We report on systematic investigations of the diameter-dependence of polystyrene-*block*-poly(methyl methacrylate) (PS-*b*-PMMA) nanorods, which were fabricated by melting the symmetric BCP into highly-ordered porous alumina.[9] Such moulds, which are characterised by a narrow pore size distribution and a regular arrangement of

the pores, have been employed to form 1D nanostructures from a broad range of materials.[10] Currently accessible pore diameters, D_p, range from 20 to 400 nm. Thus, D_p can be systematically varied to study whether deviations from the bulk morphology occur when the dimensions of the pores are incommensurate with the period of the BCP. Another objective of this work is to elucidate if the basic morphology type, which is determined by parameters such as the affinities of the BCP blocks to the pore walls and their relative volume fractions, is sustained under these conditions. We selected PS-*b*-PMMA[1] because this BCP has attracted a great deal of interest for nanotechnological applications. An example is the preparation of ordered porous PS films by selectively removing PMMA using UV light.[11] To probe the morphology of the PS-*b*-PMMA nanorods, we released them from the templates, selectively stained the PS-rich domains and investigated ultra-thin sections of the nanorods embedded in epoxy resin by means of transmission electron microscopy (TEM).

Experimental Part

The details on the preparation of self-ordered porous alumina are discussed elsewhere.[9] We used PS($\overline{M}_w = 38\,000$)-*b*-PMMA($\overline{M}_w = 36\,800$) diBCP with an overall weight average molecular weight $\overline{M}_w$ of 74 800 $g \cdot mol^{-1}$ (polydispersity index = 1.08), which was obtained from Polymer Source, Inc. The volume fractions occupied by the PS and PMMA blocks were both 50 vol.-%. The ordered porous alumina templates were placed in a furnace at a temperature of 200 °C in an argon atmosphere. The BCP powder was placed on the surface of the templates and rubbed into the pores. The samples were then cooled to 180 °C at a rate of 1.3 $K \cdot min^{-1}$ and annealed under vacuum at this temperature for 24 h. After removing the samples from the furnace, their surfaces were carefully cleaned with a sharp blade. Then, the aluminium substrates, to which the porous alumina layers had been attached, were selectively etched with a solution containing 6.8 g copper(II) chloride dihydrate ($CuCl_2 \cdot 2H_2O$), 200 ml 37% HCl and 200 ml deionised water. Subsequently, the alumina membranes were rinsed with water and dissolved in 30 wt.-% aqueous KOH at room temperature to release the BCP nanostructures. The exposure time should be kept below 1 h in order to prevent the formation of insoluble aluminium hydroxides. The suspensions containing the BCP nanostructures were washed several times with deionised water and ethanol by centrifuging and subsequent removal of the supernatant solution. The ethanolic suspension of the nanorods thus obtained was dropped in one of the compartments of a two-compartment glass container, and the solvent was evaporated. Then, we added a few droplets of a solution of 0.2 g ruthenium chloride hydrate ($RuCl_3 \cdot 3H_2O$, purchased from Aldrich) in 10 ml 10 wt.-% sodium hypochlorite (NaOCl, purchased from Aldrich)[12] into the second compartment and sealed the container. After a few seconds the colour of the BCP nanostructures turned to black. The in situ formed volatile RuO_4, which is transported via the gas phase, exclusively stains PS, whereas PMMA remains unaltered.[13] The staining solution was removed after an exposure time of approximately 30 s, and the BCP nanostructures were again suspended in ethanol. An aliquot was transferred into moulds, embedded in epoxy resin (Durcupan ACM) and cured at 65 °C for 48 h. Slices with a thickness of 70 nm or less, as obvious from their interference colours, were prepared using an ultramicrotome equipped with a diamond knife. The slices were transferred onto copper grids with holey carbon films for the TEM investigations, which were performed with a JEM 1010 operated at an accelerating voltage of 100 kV.

Results and Discussion

We prepared the BCP nanorods by melting symmetric PS-*b*-PMMA with a bulk period of 39 nm on the surface of self-ordered porous alumina with D_p-values of 25, 60, 180 and 400 nm, respectively, and a pore depth of 100 μm. Such templates are characterised by a polycrystalline degree of order, i.e., the self-ordered domains possess a lateral extension in the micron range. Employing self-ordered porous alumina is particularly attractive because the pores have a well-defined shape with a constant diameter over their entire depth. The pore size distribution is rather narrow: its dispersity, which is calculated by dividing the standard deviation by the mean pore diameter, amounts to 8% compared to at least 20% in case of commercially available porous alumina. Figure 1a shows, for example, a scanning electron microscopy (SEM) image of the surface of an ordered porous alumina template ($D_p = 400$ nm).

For the TEM investigations we prepared ultra-thin slices of specimens containing the released BCP nanorods embedded in epoxy resin. Because of their random distribution the long axes of some nanorods were oriented perpendicularly, and those of some others parallel to the direction of cutting. Precisely cutting perpendicularly to the long and short axes of the nanorods is rather difficult. Thus, most of the cross-sections across the nanorods are rather elliptical than circular, and those parallel to their long axes often do not meet the middle of the nanorods. One would not be able to

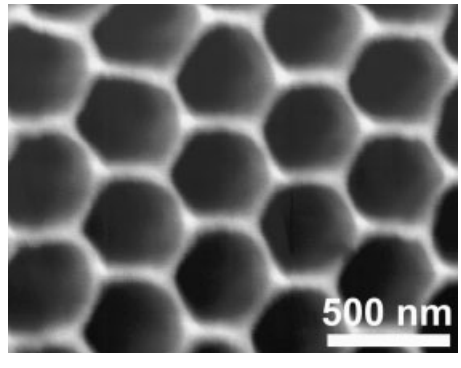

Figure 1. Scanning electron microscopic (SEM) image (top view) of self-ordered porous alumina ($D_p = 400$ nm).

distinguish between PS- and PMMA-rich domains if one investigated unstained samples. Therefore, we selectively stained the PS-rich domains with RuO_4. After this treatment they appear considerably darker than the PMMA domains because of the mass thickness contrast of the heavy Ru atoms.[13] Moreover, the PS-rich regions were apparently thicker than the PMMA-rich ones. This phenomenon can be explained by the volume expansion of the PS domains upon staining and irradiation-induced thinning of the PMMA domains.[14]

Figure 2 represents the thus obtained TEM micrographs. Figure 2(a–b) show cross-sections perpendicular to the long axes of nanorods, which were released from ordered porous alumina with $D_p = 400$ nm. In the ellipse represented in Figure 2a five dark concentric rings occur, whereas the core is bright (note that the outermost rings were partially destroyed in the course of the sample preparation). In Figure 2b four dark concentric rings and a dark core are discernible. The sections parallel to the long axes of the nanorods, as the one depicted in Figure 2c, also show dark stripes aligned to the long axes. The actual values of the numbers of lamellae and the fibre diameter are larger than the apparent ones because the cross-section shown does not meet the middle of the fibre. However, in agreement with previous theoretical work[6,7] these results indicate the presence of lamellae in the form of hollow cylinders parallel to the long axes of the nanorods. As D_p of the templates used as moulds is decreased to 180 nm, the number of rings also decreases. Either two concentric black rings (Figure 2d) or a solid black core surrounded by two concentric black rings (Figure 2e) occur in the cross-sections perpendicular to the long axes. Correspondingly, the cross-sections parallel to the long axes show four (Figure 2f) or five (Figure 2g) dark stripes, which are aligned with the long axes.

To study the microphase separation for D_p-values close to or even less than the bulk period of 39 nm, we used templates with $D_p = 60$ nm and $D_p = 25$ nm (Figure 3). Figure 3a displays cross-sections perpendicular, and Figure 3b parallel to the long axes of nanorods liberated from porous alumina with $D_p = 60$ nm. The nanorods in Figure 3a only

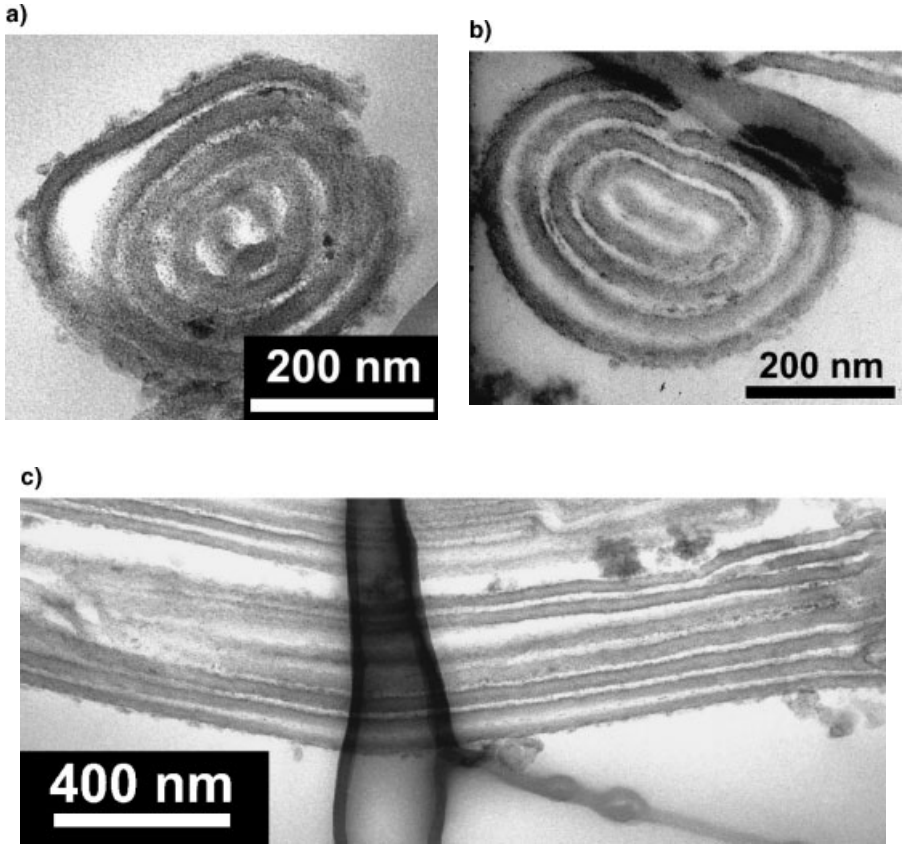

Figure 2. Transmission electron microscopic (TEM) images of ultra-thin slices containing cross-sections of polystyrene-*block*-poly(methyl methacrylate) (PS-*b*-PMMA) nanorods embedded in epoxy resin after selectively staining the PS-rich domains with RuO_4; a, b: cross-sections perpendicular to the long axes of nanorods released from templates with $D_p = 400$ nm; c: cross-section parallel to the long axis of a nanorod released from a template with $D_p = 400$ nm; d, e: cross-sections perpendicular to the long axes of nanorods released from templates with $D_p = 180$ nm; f, g: cross-sections parallel to the long axes of nanorods released from templates with $D_p = 180$ nm.

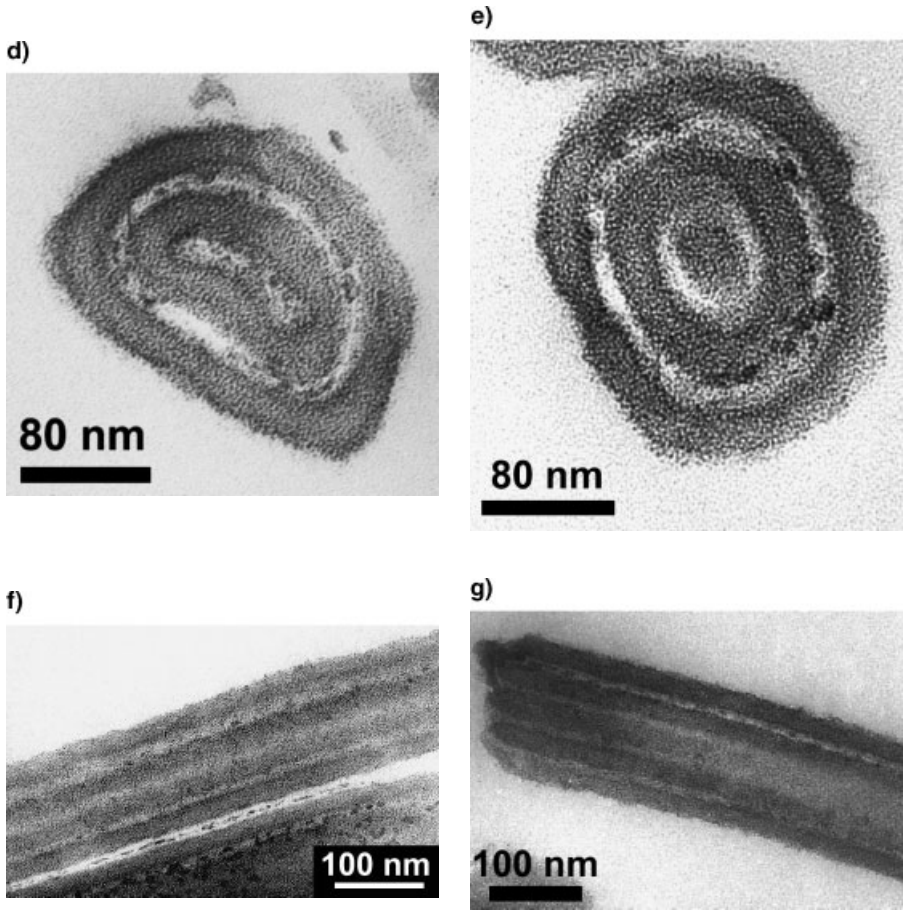

Figure 2. (*Continued*)

comprise one black ring, and correspondingly two black stripes per fibre appear in Figure 3b. Figure 3c represents cross-sections across, and Figure 3d along nanorods prepared using templates with $D_p = 25$ nm. Only one solid black circle or stripe, respectively, occurs per nanorod.

Previous theoretical investigations revealed that a liquid/liquid decomposition of a binary system confined to a cylindrical pore is strongly affected by the interactions between the critical components and the non-critical pore walls.[15] If both components have equal affinities to them, a phase separation should lead to a non-wetting morphology where both phases are in contact with the neutral pore walls. If one component exhibits a significantly stronger affinity, the phase in which this component is enriched will exclusively wet the pore walls, which thus have a non-neutral character. For both PMMA/PS homopolymer blends and PS-*b*-PMMA, a preferential segregation of the PMMA to inorganic oxide surfaces, such as alumina, has been generally observed.[16] Therefore, we assume that the PMMA forms the outermost layer of the PS-*b*-PMMA nanorods, which is in exclusive contact with the pore walls. However, in the TEM micrographs this PMMA lamella surrounding the PS layer on the apparent outside of the released BCP nanostructures, cannot be distinguished from the surrounding epoxy resin.

According to the predictions by He et al.[6] and Fraaije et al.[7], one would expect the formation of lamellae in the form of concentric cylinders aligned with the long axes of the pores, which are alternately composed of PMMA and PS. The experimental results shown in Figure 2 and 3 are summarised in Figure 4, which sketches schematic cross-sections of the nanorods perpendicular to their long axes. In case of the nanorods having D_p-values of 400, 180 and 60 nm, which are larger than the repeat period of the BCP, the presence of stained and unstained areas clearly evidences the formation of ordered states. Their morphology is characterised by cylindrical features parallel to their long axes. The lamellae form hollow cylinders, whose number decreases as D_p decreases. At first glance one would assume that the bulk period of 39 nm is commensurate with a D_p-value of 400 nm, that is, exactly 10 periods would fit into the cross-section of the pore. However, each period comprises one PMMA and one PS lamella. Because the outermost PMMA layer encloses the entire circumference of the nanorods, the number of PMMA layers along their diameters must be larger by one than the number of PS layers.

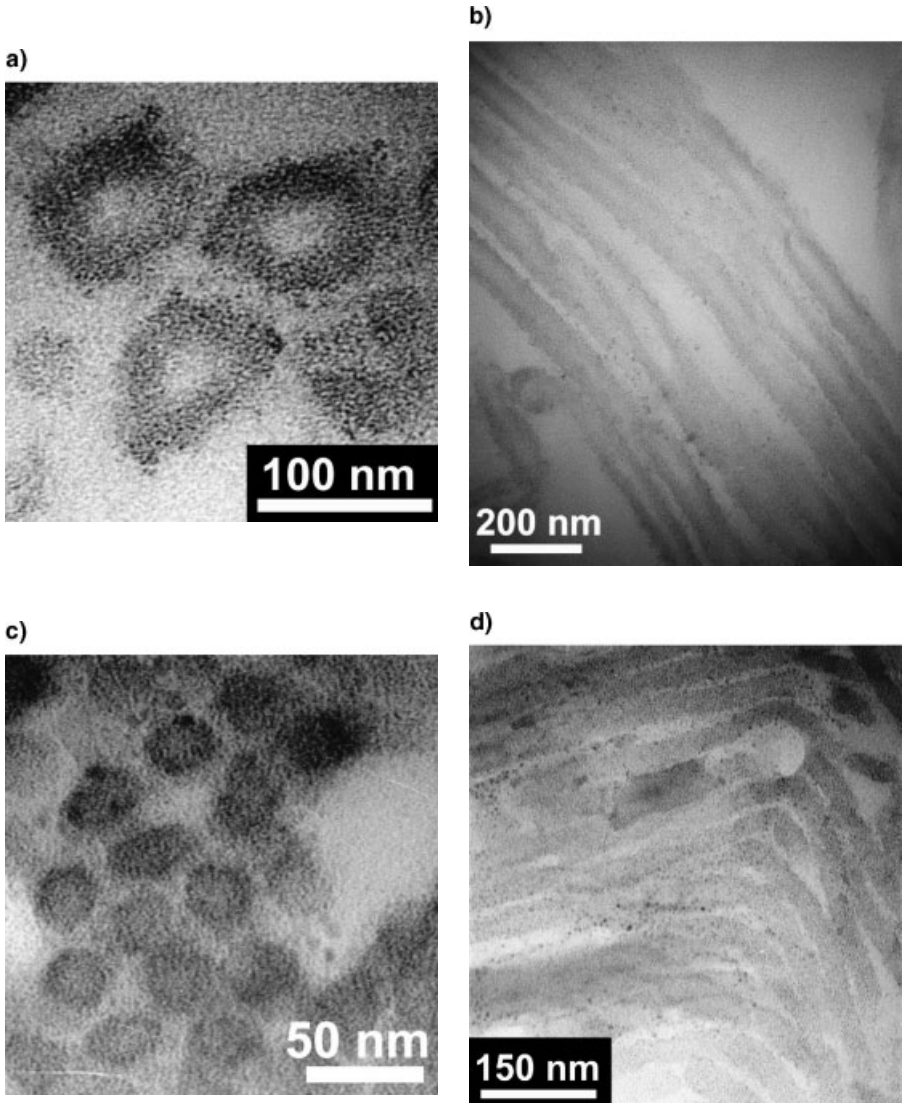

Figure 3. TEM images of ultra-thin slices containing cross-sections of PS-*b*-PMMA nanorods with diameters close or below their bulk period, embedded in epoxy resin after selectively staining the PS-rich domains with RuO_4; a: cross-sections perpendicular to the long axes of nanorods released from templates with $D_p = 60$ nm; b: cross-sections parallel to the long axes of nanorods released from templates with $D_p = 60$ nm; c: cross-sections perpendicular to the long axes of nanorods released from templates with $D_p = 25$ nm; d: cross-sections parallel to the long axes of nanorods released from templates with $D_p = 25$ nm.

Therefore, the pores cannot accommodate an integer number of periods, but only an odd number of 'half periods'. If the PMMA forms the core of the nanorods, i.e., the innermost layer, the number of the PMMA lamellae is odd and the one of the PS lamellae even. Vice versa, the number of the PMMA layers is even and the one of the PS layers odd if the PS forms the core.

If one considers the overall number of lamellae within one pore, one should take into account that even in case of ordered porous alumina deviations from the mean D_p-value occur. Moreover, staining and mechanical deformation during the preparation of the ultra-thin slices may give rise to changes of the apparent layer thickness. These problems complicate the quantitative evaluation of the domain structures. In the case of 400 nm nanorods we found either 10.5 or 9.5, in the case of 180 nm nanorods either 5.5 or 4.5 and for 60 nm nanorods 2.5 periods along their diameter. The 60 nm nanorods consist of a three-layer structure in which an outermost PMMA cylinder surrounds a PS cylinder, which in turn surrounds a PMMA core. In the case of nanorods with a D_p-value of 25 nm considerable deviations from the bulk behaviour must occur. Their morphology may be characterised either by 'ordered' cylindrical lamellae oriented parallel to the long axes of the pores, where PMMA

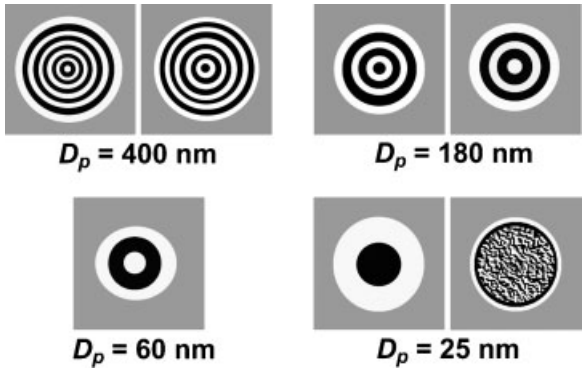

Figure 4. Schematic representation of the morphologies of PS-*b*-PMMA nanorods prepared within ordered porous alumina with different D_p-values. The figure sections sketch cross-sections perpendicular to the long axes of the nanorods and template pores, respectively. The black areas denote the PS-rich and the white ones the PMMA-rich phases. The grey areas represent the alumina pore walls.

forms the shell and PS the core, or a disordered state similar to the scenario discussed by He et al.[6] In the latter case, the BCP/pore wall interactions should nevertheless result in a preferential segregation of the PMMA to the pore walls, and next to the PMMA wetting layer there would be a PMMA depletion layer, where in turn PS was enriched. Both scenarios are schematically represented in Figure 4. A careful examination of Figure 3c reveals that the staining is somewhat heavier on the outside of the nanorods. This might be a signature of a PS-rich PMMA depletion layer, indicating the enrichment of PMMA on the pore walls. The results are, however, ambiguous. Yet, neither interpretation can be ruled out on the basis of our experimental data. Particularly the influence of the curvature of the pore walls on the morphology of the nanorods has to be addressed in future studies.

Conclusion

We have investigated the diameter-dependence of the morphology of symmetric PS-*b*-PMMA confined to the pores of highly ordered porous alumina templates. For this purpose, the diameters of the template pores were systematically varied from 25 to 400 nm. The thus produced nanorods consist of cylindrical lamellae oriented parallel to the long axes of the pores when their diameter exceeds the BCP period. The overall number of lamellae decreases as D_p decreases. Because PMMA should segregate to the pore walls, forming the outermost lamella enclosing the entire circumference of the nanorods, the pores cannot accommodate an integer number of repeat periods. An odd number of half periods alternately containing either one PS or PMMA layer occur along the pore diameter. If the pore diameter is smaller than the repeat period, a PS-containing core occurs, and one arrives at a core/shell-type morphology. It is, however, difficult to judge whether or not this structure corresponds to an ordered state. BCPs may form 1D nano-objects with complex self-ordered fine structures even if the guiding geometry is not commensurate with the BCP bulk period. Tailoring the volume fraction ratio of the blocks and the molecular architecture should allow for the design of sophisticated mesoscopic architectures as already demonstrated by Shin et al.[8] One phase could be selectively loaded with nanoparticles or inorganic functional materials, so that, for instance, nano-capacitors or nano-cables can be fabricated. Porous BCP nanorods could be obtained by selectively removing one component, such as PMMA from PS-*b*-PMMA. Currently, however, only the very first steps toward the exploration of this promising class of hierarchical nanomaterials have been taken.

Acknowledgements: The authors would like to thank Mr. *Silko Grimm* for the preparation of ordered porous alumina templates and Ms. *Rosamunde Möhner* for performing ultra-microtomy.

[1] [1a] F. S. Bates, G. H. Fredrickson, *Annu. Rev. Phys. Chem.* **1990**, *41*, 525; [1b] C. Park, J. Yoon, E. L. Thomas, *Polymer* **2003**, *44*, 6725; [1c] M. Lazzari, M. A. Lopez-Quintela, *Adv. Mater.* **2003**, *15*, 1583; [1d] "*Developments in Block Copolymer Science and Technology*", I. W. Hamley, Ed., Wiley, Chichester, UK 2004.
[2] [2a] T. L. Morkved, M. Lu, A. M. Urbas, E. E. Ehrichs, H. M. Jaeger, P. Mansky, T. P. Russell, *Science* **1996**, *273*, 931; [2b] J. P. Spatz, A. Roescher, M. Möller, *Adv. Mater.* **1996**, *8*, 337; [2c] M. Park, C. Harrison, P. M. Chaikin, R. A. Register, D. H. Adamson, *Science* **1997**, *276*, 1401; [2d] M. Muthukumar, C. K. Ober, E. L. Thomas, *Science* **1997**, *277*, 1225; [2e] T. Thurn-Albrecht, J. Schotter, G. A. Kästle, N. Emley, T. Shibauchi, L. Krusin-Elbaum, K. Guarini, C. T. Black, M. T. Tuominen, T. P. Russell, *Science* **2000**, *290*, 2126; [2f] G. Krausch, R. Magerle, *Adv. Mater.* **2002**, *14*, 1579.
[3] [3a] C. Wu, M. Li, S. Chi Man Kwan, G. J. Liu, *Macromolecules* **1998**, *31*, 7553; [3b] G. J. Liu, X. Yan, S. Duncan, *Macromolecules* **2002**, *35*, 9788.
[4] C. R. Martin, *Science* **1994**, *266*, 1961.
[5] H. Q. Xiang, K. Shin, T. Kim, S. I. Moon, T. J. McCarthy, T. P. Russell, *Macromolecules* **2004**, *37*, 5660.
[6] X. He, M. Song, H. Liang, C. Pan, *J. Chem. Phys.* **2001**, *114*, 10510.
[7] G. J. A. Sevink, A. V. Zvelindovsky, J. G. E. M. Fraaije, H. P. Huinink, *J. Chem. Phys.* **2001**, *115*, 8226.
[8] K. Shin, H. Xiang, S. I. Moon, T. Kim, T. J. McCarthy, T. P. Russell, *Science* **2004**, *306*, 76.
[9] [9a] H. Masuda, K. Fukuda, *Science* **1995**, *268*, 1466; [9b] H. Masuda, M. Satoh, *Jpn. J. Appl. Phys.* **1996**, *35*, L126; [9c] H. Masuda, F. Hasegawa, S. Ono, *J. Electrochem. Soc.* **1997**, *144*, L127; [9d] H. Masuda, K. Yada, A. Osaka, *Jpn. J. Appl. Phys. Part 2* **1998**, *37*, L1340; [9e] K. Nielsch, J. Choi, K. Schwirn, R. B. Wehrspohn, U. Gösele, *Nano Lett.* **2002**, *2*, 677.
[10] [10a] D. H. Kim, P. Karan, P. Göring, J. Leclaire, A.-M. Caminade, J.-P. Majoral, U. Gösele, M. Steinhart, W. Knoll,

Small **2005**, *1*, 99; [10b] P. Göring, E. Pippel, H. Hofmeister, R. B. Wehrspohn, M. Steinhart, U. Gösele, *Nano Lett.* **2004**, *4*, 1121; [10c] Y. Luo, S. K. Lee, H. Hofmeister, M. Steinhart, U. Gösele, *Nano Lett.* **2004**, *4*, 143; [10d] M. Steinhart, Z. Jia, A. K. Schaper, R. B. Wehrspohn, U. Gösele, J. H. Wendorff, *Adv. Mater.* **2003**, *15*, 706; [10e] M. Steinhart, J. H. Wendorff, A. Greiner, R. B. Wehrspohn, K. Nielsch, J. Schilling, J. Choi, U. Gösele, *Science* **2002**, *296*, 1997; [10f] M. Steinhart, S. Senz, R. B. Wehrspohn, U. Gösele, J. H. Wendorff, *Macromolecules* **2003**, *36*, 3646; [10g] M. Steinhart, R. B Wehrspohn, J. H. Wendorff, *Chem. Phys. Chem.* **2003**, *4*, 1171.

[11] [11a] P. Mansky, Y. Liu, E. Huang, T. P. Russell, C. Hawker, *Science* **1997**, *275*, 1458; [11b] K. W. Guarini, C. T. Black, K. R. Milkove, R. L. Sandstrom, *J. Vac. Sci. Technol. B* **2001**, *19*, 2784; [11c] K. W. Guarini, C. T. Black, S. H. I. Yeung, *Adv. Mater.* **2002**, *14*, 1290.

[12] Martin Kunz, Ph.D. thesis, Albert-Ludwigs-University, Freiburg 1990, p. 208.

[13] J. S. Trent, J. I. Scheinbeim, P. R. Couchman, *Macromolecules* **1983**, *16*, 589.

[14] B. H. Sohn, S. H. Yun, *Polymer* **2002**, *43*, 2507.

[15] [15a] A. J. Liu, D. J. Durian, E. Herbolzheimer, S. A. Safran, *Phys. Rev. Lett.* **1990**, *65*, 1897; [15b] Z. P. Zhang, A. Chakrabarti, *Phys. Rev. E* **1994**, *50*, R4290; [15c] L. D. Gelb, K. E. Gubbins, *Physica A* **1997**, *244*, 112; [15d] L. D. Gelb, K. E. Gubbins, *Phys. Rev. E* **1997**, *55*, R1290; [15e] K. Binder, J. Non-Equilib, *Thermodyn.* **1998**, *23*, 1; [15f] L. D. Gelb, K. E. Gubbins, R. Radhakrishnan, M. Sliwinska-Bartkowiak, *Rep. Prog. Phys.* **1999**, *62*, 1573.

[16] [16a] S. Walheim, M. Böltau; J. Mlynek, G. Krausch, U. Steiner, *Macromolecules* **1997**, *30*, 4995; [16b] E. Buck, J. Fuhrmann, *Macromolecules* **2001**, *34*, 2172; [16c] M. Harris, G. Appel, H. Ade, *Macromolecules* **2003**, *36*, 3307.

